

Finslerian wormholes in squared trace gravity

Z. Nekouee* ¹, B. R. Yashwanth † ², Manjunath Malligawad ‡ ³, S. K. Narasimhamurthy § ⁴, S. K. J. Pacif ¶ ^{5,6} and Kazuharu Bamba ** ⁷

¹*School of Physics, Damghan University, Damghan, 3671641167, Iran*

²*Department of Mathematics, Mangalore Institute of Technology & Engineering, Badaga Mijar, Moodabidri, Mangalore-574225, Karnataka, India*

³*Department of Mathematics, Sri Siddhartha Institute of Technology, A Constituent College of Siddhartha Academy of Higher Education, Tumkur-572105, Karnataka, India.*

⁴*Department of PG Studies and Research in Mathematics, Kuvempu University, Jnana Sahyadri, Shankaraghatta-577 451, Shivamogga, Karnataka, India*

⁵*Pacif Institute of Cosmology and Selfology (PICS), Sagara, Sambalpur-768 224, Odisha, India*

⁶*Research Center of Astrophysics and Cosmology,*

Khazar University, Baku, AZ1096, 41 Mehseti Street, Azerbaijan

⁷*Faculty of Symbiotic Systems Science, Fukushima University, Fukushima 960-1296, Japan*

We investigate traversable wormholes in squared-trace extended gravity within the framework of Finsler-Randers geometry equipped with the Barthel connection. The Einstein–Hilbert action is modified by terms involving the trace of the energy–momentum tensor and its square, generating effective anisotropies through matter–curvature coupling. The resulting field equations are studied under barotropic equations of state with exponential and power-law shape functions. Finslerian anisotropy introduces novel pressure dynamics that enable the classical energy conditions to be satisfied in specific parameter domains. Our analysis shows that the Barthel connection significantly extends the parameter space for non-exotic, physically viable wormholes compared to purely Riemannian models. These findings suggest that Finslerian modifications provide a powerful mechanism for realizing realistic wormhole structures, offering new perspectives on anisotropic and geometrically enriched space-time configurations in extended gravity.

I. INTRODUCTION

The idea of traversable wormholes, idealized channels between separate regions of space-time, has intrigued physicists since their theoretical construction in general relativity (GR) [1, 2]. Within the standard GR context, these wormholes usually require the use of exotic matter that breaks the null energy condition (NEC) to stabilize geometry [3, 4]. Nevertheless, exotic matter is hypothetical, and its inconsistency with established physics has driven the study of alternative theories of gravity to create wormholes without contradicting the energy conditions [5]. Among all the modified theories [6–14], $f(\mathbb{R}, \mathbb{T})$ gravity has received significant interest, where \mathbb{R} is the Ricci scalar and \mathbb{T} represents the trace of the energy-momentum tensor.

This requirement severely limits the physical plausibility of the geometries. Alternative theories of gravity provide a natural means of relaxing this constraint by altering the effective gravitational dynamics, thereby allowing the support of wormhole structures with minimal or no exotic matter. One auspicious approach arises within

the $f(\mathbb{R}, \mathbb{T})$ class of theories [15], in which the gravitational Lagrangian depends not only on the Ricci scalar, but also on the trace of the energy–momentum tensor [16–18]. This matter-geometry coupling introduces extra degrees of freedom that can modify the effective energy-momentum tensor seen by the geometry, allowing the energy conditions to be satisfied under suitable circumstances [19]. A notable extension of this framework is the so-called *squared trace-extended gravity* [20–22], characterized by $f(\mathbb{R}, \mathbb{T}) = \mathbb{R} + \ell_1 \mathbb{T} + \ell_2 \mathbb{T}^2$, where ℓ_1 and ℓ_2 are coupling constants controlling the strength of the linear and quadratic trace contributions. The presence of the quadratic \mathbb{T}^2 term represents higher-order matter corrections to the gravitational action. This addition plays a crucial role: it offers enhanced flexibility in tailoring the effective stress-energy tensor, thereby expanding the parameter space in which NEC, as well as other classical energy conditions (weak, dominant, and strong), can be satisfied while maintaining the flaring-out condition at the wormhole throat [23, 24].

Within this setting, a variety of shape functions, such as power-law or exponential profiles, can be employed along with different matter configurations, including anisotropic fluids and barotropic equations of state of the form $p_r = \omega_r \rho$ and $p_t = \omega_t \rho$ [25]. Model’s viability depends sensitively on the choice of coupling constants, matter distribution, and equation of state (EoS) parameters. For suitable choices, asymptotically flat wormhole geometries have been realized that remain entirely supported by non-exotic matter throughout the space-time.

*zohrehnekouee@gmail.com

†yashmath0123@gmail.com

‡manjunathmalligawad91@gmail.com

§nmurthysk@gmail.com

¶shibesh.math@gmail.com

**bamba@sss.fukushima-u.ac.jp

From a broader perspective, the $\mathbb{R} + \ell_1 \mathbb{T} + \ell_2 \mathbb{T}^2$ framework stands out among alternative theories of gravity for wormhole physics because it achieves this balance without resorting to elaborate curvature invariants or higher-derivative terms in \mathbb{R} . Its appeal lies in its minimal modification to GR, its capacity to incorporate realistic matter sources, and its potential to reconcile the existence of traversable wormholes with the known energy conditions - an outcome unattainable in standard GR.

A key mathematical feature of squared trace-extended gravity is its field equations, which include higher-order corrections to matter content. In this theory, the effective Einstein field equations are [26]: $\mathbb{G}_{\mu\nu} = 8\pi\mathbb{T}_{\mu\nu}^{\text{eff}}$, where the effective energy-momentum tensor $\mathbb{T}_{\mu\nu}^{\text{eff}}$ includes both standard and trace-corrected contributions. The addition of quadratic \mathbb{T} terms introduces further nonlinearities into the field equations, necessitating a careful choice of the redshift and shape functions to ensure solvability. These nonlinearities also open the possibility of anisotropic pressures that are compatible with energy conditions, an outcome that is not easily achievable in GR.

One persuasive reason for exploring squared trace terms is the field of cosmology. It has been established that theories of this form can cause cosmic acceleration at later times and prevent Big Bang singularities [27]. This dual utility in both cosmological and astrophysical contexts attests to the theoretical strength of the squared trace gravity.

In short, traversable wormholes in squared trace-extended gravity are an exciting route for achieving stable and physically viable wormhole geometries without the need to invoke exotic matter [25, 28]. This theoretical development holds new promise for the physics of wormholes and further enlightens our comprehension of how gravity could behave outside the reach of GR.

New progress in Finsler geometry, especially within the framework of the Barthel connection formalism, presents an attractive context for investigating space-time anisotropies [29–31]. Finslerian generalizations of gravity theories are a natural arena for incorporating direction-dependent phenomena that do not exist in Riemannian geometry per se. Here, the squared trace alternative theory of gravity may be supplemented by Barthel–Finsler structures to encapsulate more general wormhole geometries that can incorporate anisotropic pressure distributions and non-trivial topologies. With this motivation in mind, the conventional $\mathfrak{f}(\mathbb{R}, \mathbb{T})$ wormhole analysis can be extended to the Barthel–Finsler context, wherein the connection and curvature are no longer restricted under Riemannian symmetry. This geometric extension allows for the construction of wormhole solutions that can be more physically realistic and potentially provide a deeper understanding of matter-geometry couplings under anisotropic conditions; however, this area has not been fully explored in the current literature.

In summary, studying wormhole space-times does not replace black hole physics; instead, it enriches it. They provide a horizon-free, topologically nontrivial, anisotropic arena in which the role of energy conditions, matter–geometry coupling, and causal structure can be explored with unprecedented clarity. From this perspective, wormholes are not merely speculative geometries but indispensable tools for deducing the limits of classical general relativity and the viability of its extensions in the strong-gravity regime.

Despite these advances, wormhole solutions in Riemannian $\mathfrak{f}(\mathbb{R}, \mathbb{T})$ and related modified gravity theories often remain viable only within narrow regions of the equation-of-state parameter space, particularly when classical energy conditions are imposed. In many cases, NEC-satisfying configurations require fine-tuned matter distributions or are restricted to specific choices of shape functions. This limitation motivates the exploration of geometric generalizations beyond the Riemannian framework. In this context, Finsler–Randers geometry offers a natural extension in which space-time anisotropy arises intrinsically from the geometry itself, providing a promising avenue for enlarging the physically admissible parameter space of wormhole solutions.

The remainder of this paper is organized. In Sec. II, we introduce the geometric features of Barthel connections in Finsler spaces. Sec. III describes the development of the basic framework of $\mathfrak{f}(\mathbb{R}, \mathbb{T})$ gravity and the associated field equations. The wormhole configurations and energy condition analyses using the two shape functions in the Finsler framework are detailed in Secs. IV and V. Sec. VI highlights the role of exotic matter in maintaining traversable wormholes, while Sec. VII presents concluding remarks.

II. GEOMETRIC STRUCTURES INDUCED BY BARTHEL CONNECTIONS IN FINSLER SPACES

Consider a smooth Finsler metric \mathbb{F} on a differentiable manifold \mathbb{M} , equipped with local coordinates (x^i, y^i) on the tangent bundle $\mathbb{T}\mathbb{M}$. The components of the metric tensor are expressed as:

$$\mathfrak{g}_{\iota\varsigma} = \mathbb{F}\mathbb{F}_{y^\iota y^\varsigma} + \mathbb{F}_{y^\iota} \mathbb{F}_{y^\varsigma}, \quad (1)$$

with $\mathbb{F}_{y^\iota} = \frac{\partial \mathbb{F}}{\partial y^\iota}$.

In the realm of Finsler geometry, metrics of the (α, β) -type represent spaces constructed from a Riemannian metric $\alpha(x, y)$ combined with a 1-form $\beta(x, y)$. This setup differentiates them from traditional Riemannian geometries. Notable instances include Randers and Kropina metrics [32, 33]. The Riemannian element α captures isotropic, spherically symmetric aspects, whereas the 1-form β incorporates directional variations [34]. The Randers metric takes the form:

$$\mathbb{F}(x, y) = \alpha(x, y) + \beta(x, y) = \sqrt{\mathfrak{a}_{\iota\varsigma} y^\iota y^\varsigma} + \mathbb{A}_\nu(x) y^\nu. \quad (2)$$

This research aims to explore Finslerian applications in cosmological scenarios, emphasizing wormhole structures via Randers formalism. Notably, spatial coordinates are treated as comoving, and the time coordinate aligns with proper time observed by comoving entities. Inserting Eq. (2) into Eq. (1), assuming $\mathbb{L} = \frac{1}{2}\mathbb{F}^2$, produces:

$$\begin{aligned} \mathfrak{g}_{\nu\zeta}(x, y) &= \frac{\mathbb{L}_{\alpha}}{\alpha} \mathfrak{a}_{\nu\zeta} + \frac{\mathbb{L}_{\alpha\alpha}}{\alpha^2} y_{\nu} y_{\zeta} + \frac{\mathbb{L}_{\alpha\beta}}{\alpha} (\mathbb{A}_{\nu} y_{\zeta} + \mathbb{A}_{\zeta} y_{\nu}) \\ &+ \mathbb{L}_{\beta\beta} \mathbb{A}_{\nu} \mathbb{A}_{\zeta} - \frac{\mathbb{L}_{\alpha}}{\alpha^3} y_{\nu} y_{\zeta}. \end{aligned} \quad (3)$$

Similar to Riemannian settings, covariant derivatives in Finsler geometry rely on connections. However, Finsler manifolds support multiple connection types, highlighting their structural diversity [32, 35–37]. This variety facilitates advanced geometric studies but poses challenges for cohesive theoretical models due to computational and interpretative complexities.

The Barthel connection was developed to address limitations in the Berwald connection and refine elements of the Cartan connection [35]. The configuration $(\mathbb{M}, \mathbb{F}(x, y), \mathbb{Y}(x))$ includes a Finsler manifold $(\mathbb{M}, \mathbb{F}(x, y))$ paired with a vector field $\mathbb{Y}(x)$ on \mathbb{M} . Requiring $\mathbb{Y}(x) \neq 0$ everywhere in \mathbb{M} transforms the induced metric into a \mathbb{Y} -Riemannian form. The fundamental tensor yields the \mathbb{Y} -tensor field, defining the \mathbb{Y} -Riemannian structure. Compatible with the Finsler metric, the Barthel connection features a torsion tensor that maintains vector magnitudes during parallel translation, proving beneficial for physical applications. It enables viewing Finsler manifolds as point-wise structures with local Minkowski-like (non-Euclidean) properties. For (α, β) -based Finsler metrics, the Barthel linear connection—derived from the Cartan connection—functions as the Levi-Civita connection for the associated \mathbb{Y} -Riemannian manifold [38]. This setup also connects to the linear \mathbb{Y} -connection, formed via the Cartan connection and a smooth, nonzero vector field $\mathbb{Y}(x)$ (further details available in [38–40]).

Next, we examine the osculating Riemannian metric stemming from the Finsler metric (\mathbb{M}, \mathbb{F}) . As previously noted, primary Finsler geometric elements reside on the total space $\mathbb{T}\mathbb{M}$ of the tangent bundle, with projection $\pi_{\mathbb{M}} : \mathbb{T}\mathbb{M} \rightarrow \mathbb{M}$. This space forms a $2n$ -dimensional smooth manifold, described by local coordinates (x^i, y^i) . Here, $x = (x^i)$ and $y = (y^i)$ are independent variables. For example, the metric tensor $\mathfrak{g}_{ij} : \mathbb{T}\mathbb{M} \setminus \mathbb{O} \rightarrow \mathbb{R}$ is specified on the tangent bundle excluding the zero section \mathbb{O} . The projection $\pi_{\mathbb{M}} : \mathbb{T}\mathbb{M} \rightarrow \mathbb{M}$ establishes a fiber bundle, allowing a local section $\mathbb{Y} : \mathbb{U} \rightarrow \mathbb{T}\mathbb{U}$, where $\mathbb{U} \subset \mathbb{M}$ is open and $\mathbb{Y}(x) \neq 0$ for $x \in \mathbb{U}$. This satisfies $\pi_{\mathbb{M}}(\mathbb{Y}(x)) = x$. The section \mathbb{Y} facilitates pulling back geometric objects from $\mathbb{T}\mathbb{M}$ to \mathbb{M} . Thus, $\mathfrak{g}_{ij} \circ \mathbb{Y}$ acts as a tensor on \mathbb{U} , enabling the definition:

$$\mathfrak{g}_{ij}(x) := \mathfrak{g}_{ij}(x, y)|_{y=\mathbb{Y}(x)} \quad x \in \mathbb{U}. \quad (4)$$

The pair $(\mathbb{U}, \mathfrak{g}_{ij})$ constitutes a Riemannian manifold, where $\mathfrak{g}_{ij}(x) = \mathfrak{g}_{ij}(x, \mathbb{Y}(x))$ denotes the \mathbb{Y} -osculating Riemannian metric derived from the Finsler manifold (\mathbb{M}, \mathbb{F}) .

III. CONCEPTUAL FRAMEWORK

Within a geometrically modified extended theory, we consider an action featuring a non-minimal coupling between matter and curvature, expressed as

$$S = \int d^4x \sqrt{-\mathfrak{g}} \left(\frac{1}{2\chi^2} \mathfrak{f}(\mathbb{R}, \mathbb{T}) + \mathcal{L}_{\mathfrak{m}} \right). \quad (5)$$

In this setup, $\mathcal{L}_{\mathfrak{m}}$ is the matter Lagrangian, and $\chi^2 = 8\pi$. Possible forms of the matter Lagrangian include $\mathcal{L}_{\mathfrak{m}} = -\mathbb{T}$, $\mathcal{L}_{\mathfrak{m}} = -\rho$, and $\mathcal{L}_{\mathfrak{m}} = \mathfrak{p}$, with $\mathfrak{p} = \frac{p_r + 2p_t}{3}$ representing the average pressure. Here, we consider $\mathcal{L}_{\mathfrak{m}} = \mathfrak{p}$ as it provides a natural and physically consistent choice. The connection between the matter Lagrangian and the energy-momentum tensor arises through the variational principle, leading to the expression,

$$\mathbb{T}_{\mu\nu} = -\frac{2}{\sqrt{-\mathfrak{g}}} \frac{\delta(\sqrt{-\mathfrak{g}} \mathcal{L}_{\mathfrak{m}})}{\delta \mathfrak{g}^{\mu\nu}}. \quad (6)$$

The action is generalized by introducing a function $\mathfrak{f}(\mathbb{R}, \mathbb{T})$ in place of the Ricci scalar \mathbb{R} , with \mathbb{T} being the trace of the energy-momentum tensor. For simplicity and to preserve minimal coupling, the function $\mathfrak{f}(\mathbb{R}, \mathbb{T})$ is commonly expressed as the sum $\mathfrak{f}(\mathbb{R}, \mathbb{T}) = \mathfrak{f}_1(\mathbb{R}) + \mathfrak{f}_2(\mathbb{T})$, separating curvature and matter dependencies. By performing a variation of the modified gravitational action with respect to $\mathfrak{g}_{\mu\nu}$, one obtains the field equations for the extended theory as follows [23, 25]

$$\begin{aligned} \mathbb{R}_{\mu\nu} &- \frac{\mathfrak{f}_1(\mathbb{R})}{2\mathfrak{f}_{1,1}(\mathbb{R})} \mathfrak{g}_{\mu\nu} \\ &= \frac{1}{\mathfrak{f}_{1,1}(\mathbb{R})} \left[(\nabla_{\mu} \nabla_{\nu} - \mathfrak{g}_{\mu\nu} \square) \mathfrak{f}_{1,1}(\mathbb{R}) + (\chi^2 \right. \\ &\left. + \mathfrak{f}_{2,2}(\mathbb{T})) \mathbb{T}_{\mu\nu} + \left(\mathfrak{f}_{2,2}(\mathbb{T}) \mathfrak{p} + \frac{1}{2} \mathfrak{f}_2(\mathbb{T}) \right) \mathfrak{g}_{\mu\nu} \right], \end{aligned} \quad (7)$$

for convenience, we introduced abbreviated notation for the partial derivatives with respect to the Ricci scalar \mathbb{R} and the trace \mathbb{T} of the energy-momentum tensor as follows,

$$\mathfrak{f}_{1,1}(\mathbb{R}) = \frac{\partial \mathfrak{f}_1(\mathbb{R})}{\partial \mathbb{R}}, \quad \mathfrak{f}_{2,2}(\mathbb{T}) = \frac{\partial \mathfrak{f}_2(\mathbb{T})}{\partial \mathbb{T}}. \quad (8)$$

We assume $\mathfrak{f}_1(\mathbb{R}) = \mathbb{R}$, such that the corresponding modified theory mimics GR in its field equations

$$\mathbb{G}_{\mu\nu} = (\chi^2 + \mathfrak{f}_{2,2}(\mathbb{T})) \mathbb{T}_{\mu\nu} + \left(\mathfrak{f}_{2,2}(\mathbb{T}) \mathfrak{p} + \frac{1}{2} \mathfrak{f}_2(\mathbb{T}) \right) \mathfrak{g}_{\mu\nu}, \quad (9)$$

by rewriting Eq. (9), we obtain

$$\mathbf{G}_{\mu\nu} = \varkappa_{\mathbb{T}}^2 (\mathbb{T}_{\mu\nu} + \mathbb{T}_{\mu\nu}^{\text{int}}), \quad (10)$$

where $\varkappa_{\mathbb{T}}^2 = \varkappa^2 + \mathfrak{f}_{2,2}(\mathbb{T})$, $\mathbf{G}_{\mu\nu}$ represents the Einstein tensor, with an interaction term that is expressed as follows,

$$\mathbb{T}_{\mu\nu}^{\text{int}} = \left(\frac{\mathfrak{f}_{2,2}(\mathbb{T})\mathfrak{p} + \frac{1}{2}\mathfrak{f}_2(\mathbb{T})}{\varkappa^2 + \mathfrak{f}_{2,2}(\mathbb{T})} \right) \mathfrak{g}_{\mu\nu}. \quad (11)$$

Owing to modifications in the geometry of the action, the interaction term may originate from quantum effects or imperfect fluids. Its presence implies that the non-minimal coupling between matter and geometry induces an effective matter field, which might be responsible for the late-time acceleration of the universe. It is worth noting that adopting a linear form for the functional $\mathfrak{f}_2(\mathbb{T})$ yields a constant, redefined Einstein constant $\varkappa_{\mathbb{T}}^2$. In contrast, the present study explores a quadratic form, $\mathfrak{f}_2(\mathbb{T}) = \ell_1\mathbb{T} + \ell_2\mathbb{T}^2$, which results in a \mathbb{T} -dependent Einstein constant. Here, ℓ_1 and ℓ_2 are model parameters that will be constrained based on the specific wormhole solutions under consideration. Under this choice, the interaction term takes the form,

$$\mathbb{T}_{\mu\nu}^{\text{int}} = \frac{1}{\varkappa_{\mathbb{T}}^2} \left[\ell_1 \left(\mathfrak{p} + \frac{\mathbb{T}}{2} \right) + \ell_2 \mathbb{T} \left(2\mathfrak{p} + \frac{\mathbb{T}}{2} \right) \right] \mathfrak{g}_{\mu\nu}. \quad (12)$$

Traversable wormhole solutions are typically formulated under the assumption of an anisotropic fluid, described by the energy-momentum tensor,

$$\mathbb{T}_{\mu}^{\nu} = \text{diag}(\rho, -p_r, -p_t, -p_t), \quad (13)$$

where p_r and p_t are the radial and tangential pressure components, respectively, and ρ is the energy density associated with the matter content, and the trace of the energy-momentum tensor is $\mathbb{T} = \rho - p_r - 2p_t$.

IV. FINSLERIAN PERSPECTIVES ON WORMHOLE GEOMETRY

To explore wormhole configurations within the framework of Finsler geometry using the Barthel connection, we integrate the vector field tied to the Randers structure into the general expression of the Finslerian metric. Beginning with a wormhole solution derived from

GR, we isolate its Riemannian component and introduce a 1-form to construct the corresponding Finsler-Randers geometry. Applying the osculating method to this framework yields a Barthel-type Finsler-Randers wormhole model that exhibits a Lorentzian signature. The Riemannian metric component $\alpha(x, y)$ represents spatial isotropy, while the 1-form $\beta(x, y)$ introduces directional dependence, indicating anisotropy or potential Lorentz symmetry breaking [32, 33]. Consequently, the Riemannian metric tensor \mathbf{a}_{ij} takes the form,

$$\mathbf{a}_{ij}(x) = \text{diag} \left(e^{2\Psi(r)}, -\frac{1}{1 - \frac{b(r)}{r}}, -r^2, -r^2 \sin^2 \theta \right), \quad (14)$$

based on the assumptions established in the section II, we now focus on an (α, β) -type metric and analyze the scenario where the vector field $\mathbb{Y} = \mathbb{A}$ is specified, with its components expressed as $\mathbb{A}^i = \mathbf{a}^{ij}\mathbb{A}_j$. The requirement that the vector field \mathbb{A} remains non-zero throughout the manifold \mathbb{M} implies that the 1-form β has no vanishing points. With this framework, we introduce the concept of the \mathbb{A} -osculating Riemannian manifold, denoted by $(\mathbb{M}, \mathfrak{g}_{ij})$, where the metric tensor is defined as $\mathfrak{g}_{ij}(x) := \mathfrak{g}_{ij}(x, \mathbb{A})$. Let \mathfrak{S} represent the norm of the vector field \mathbb{A} measured with respect to the Riemannian metric α , which yields the following relation,

$$\mathbb{Y}_i(x, \mathbb{A}) = \mathbb{A}_i, \quad \mathfrak{S}^2 = \mathbb{A}^i \mathbb{A}_i = \alpha^2(x, \mathbb{A}),$$

$$\beta(x, \mathbb{A}) = \mathbb{A}_i \mathbb{A}^i = \mathfrak{S}^2, \quad (15)$$

referring to Eq. (15), one finds

$$\mathfrak{g}_{ij}(x, y)|_{y=\mathbb{A}(x)} = (1 + \mathfrak{S})\mathbf{a}_{ij}(x) + \left(\frac{1}{\mathfrak{S}} + 1 \right) \mathbb{A}_i(x)\mathbb{A}_j(x). \quad (16)$$

Under the assumption that $(\mathbb{A}_i) = (\xi(r), 0, 0, 0)$, the Finsler-Barthel-Randers metric exhibits the following form

$$\alpha(x, y)|_{y=\mathbb{A}(x)} = \xi(r),$$

$$\beta(x, y)|_{y=\mathbb{A}(x)} = \xi^2(r),$$

$$\mathfrak{g}_{ij}(x, y)|_{y=\mathbb{A}(x)} = \left(1 + \xi(r) \right) \begin{bmatrix} e^{2\Psi(r)} + \xi(r) & 0 & 0 & 0 \\ 0 & -\frac{1}{1 - \frac{b(r)}{r}} & 0 & 0 \\ 0 & 0 & -r^2 & 0 \\ 0 & 0 & 0 & -r^2 \sin^2 \theta \end{bmatrix}, \quad (17)$$

with $i, j \in \{0, 1, 2, 3\}$, corresponding to $\{t, r, \theta, \phi\}$, the functions $\Psi(r)$ and $b(r)$ are interpreted as the redshift and shape functions, respectively [41]. The redshift function $\Psi(r)$ describes how redshift and tidal gravitational effects evolve with radial distance in the wormhole structure. To prevent the formation of horizons within the wormhole geometry, it is crucial that the redshift function $\Psi(r)$ remains finite throughout the space-time. The regularity of $\Psi(r)$ ensures the traversability of the wormhole, ruling out the presence of singularities or event horizons. A horizon, particularly in the case where $\Psi(r) = 0$, would obstruct bidirectional passage through the wormhole [1, 42]. This case, referred to as a tideless condition, is significant because it implies the absence of substantial tidal forces within the wormhole [41, 43, 44]. Following the motivation in Ref. [39], we consider $\xi(r)$ to be a constant. The constant ξ in the osculating Finsler-Barthel-

Randers wormhole tensor modifies the metric components, influencing curvature, gravitational strength, and wormhole features such as stability, traversability, and particle motion. It also introduces anisotropy and may reduce the need for exotic matter. Variations in ξ could lead to observable effects like lensing or redshift, while in the limit $\xi \rightarrow 0$, the metric (17) reduces to the Riemannian wormhole case.

The existence of traversable wormholes can be supported by a fluid whose radial and tangential pressures follow the barotropic relations $p_r = \varpi_1 \rho$ and $p_t = \varpi_2 \rho$, with ϖ_1 and ϖ_2 as constants of the EoS. These constants may be freely chosen or physically motivated, based on the desired scenario. Given such barotropic forms, the field equations for the traversable wormhole space-time become,

$$\frac{b'(r)}{(\xi+1)r^2} = \left[\overbrace{8\pi + \frac{\ell_1}{6}(9 - \varpi_1 - 2\varpi_2)}^{\lambda_1} \right] \rho + \left[\frac{\ell_2}{6}(1 - \varpi_1 - 2\varpi_2) \overbrace{(15 + \varpi_1 + 2\varpi_2)}^{\lambda_2} \right] \rho^2, \quad (18)$$

$$\frac{b(r)}{(\xi+1)r^3} = \left[\overbrace{-8\pi\varpi_1 + \frac{\ell_1}{6}(3 - 7\varpi_1 - 2\varpi_2)}^{\lambda_3} \right] \rho + \left[\frac{\ell_2}{6}(1 - \varpi_1 - 2\varpi_2) \overbrace{(3 - 11\varpi_1 + 2\varpi_2)}^{\lambda_4} \right] \rho^2, \quad (19)$$

$$\frac{rb'(r) - b(r)}{(\xi+1)r^3} = \left[\overbrace{-16\pi\varpi_2 + \frac{\ell_1}{3}(3 - \varpi_1 - 8\varpi_2)}^{\lambda_5} \right] \rho + \left[\frac{\ell_2}{6}(1 - \varpi_1 - 2\varpi_2) \overbrace{(6 + 2\varpi_1 - 20\varpi_2)}^{\lambda_6} \right] \rho^2. \quad (20)$$

Using Eqs. (18) and (19), one can obtain the expression for the energy density of the traversable wormhole,

$$\rho = \left[\frac{\lambda_4 r \frac{b'(r)}{b(r)} - \lambda_2}{\lambda_1 \lambda_4 - \lambda_2 \lambda_3} \right] \frac{b(r)}{(\xi+1)r^3}. \quad (21)$$

The energy density depends on both the EoS parameters and the chosen shape function of the wormhole geometry. The alternative theory of gravity under consideration introduces two arbitrary constants, ℓ_1 and ℓ_2 . Constraints on ℓ_1 , ϖ_1 , and ϖ_2 are derived directly from Eqs. (18) through (20) as follows,

$$\lambda_1 - \lambda_3 = \lambda_5, \quad (22)$$

$$\overbrace{\frac{\ell_2}{6}(1 - \varpi_1 - 2\varpi_2)}^{\chi} (\lambda_2 - \lambda_4) = \frac{\ell_2}{6}(1 - \varpi_1 - 2\varpi_2)\lambda_6. \quad (23)$$

By enforcing the condition (22), we establish a correspondence between ϖ_1 and ϖ_2 as following form,

$$\varpi_1 = -(2\varpi_2 + \gamma), \quad \gamma = \frac{6\pi}{\ell_1 + 6\pi}. \quad (24)$$

With the trace defined as $\mathbb{T} = \rho - p_r - 2p_t = (1 - \varpi_1 - 2\varpi_2)\rho$, a corresponding relation involving χ can be established as follows,

$$\chi = \frac{\ell_2 \mathbb{T}}{6 \rho}. \quad (25)$$

The condition (23), together with $\chi \neq 0$, imposes $\ell_1 = 4\pi$. Alternatively, if the trace of the matter field is zero ($\chi = 0$), the condition yields $\ell_1 = -12\pi$. To avoid a vanishing trace in our model, we consistently choose $\ell_1 = 4\pi$. The model imposes strict constraints on the numerical values of the parameters, preventing arbitrary selection. Interestingly, the energy density in the traversable wormhole model appears independent of the extended gravity

parameter ℓ_2 , while ℓ_1 can be determined through constraints from the field equations. However, an implicit dependence may still exist. Since the energy density does not explicitly involve ℓ_2 —the coupling constant associated with the squared trace term—other related quantities like pressure and energy conditions may also show no direct dependence on ℓ_2 . However, it should not be concluded that $f(\mathbb{R}, \mathbb{T})$ can take a purely linear form in \mathbb{T} . A linear choice in the current framework would yield $\chi = 0$, leading to a traceless energy-momentum tensor. To avoid this, it is essential to adopt a non-zero value for χ , which consequently requires ℓ_2 to be finite and non-zero.

V. WORMHOLE CONFIGURATIONS AND THEIR COMPATIBILITY WITH ENERGY CONDITIONS

To study non-exotic traversable wormholes under the squared trace extended gravity framework, we select two forms of the shape function: an exponential type $b(r) = re^{-2(r-r_0)}$, and a power-law type $b(r) = \sqrt{r_0 r}$, where r_0

represents the radius at the wormhole throat. It is essential to emphasize that the chosen shape functions must meet specific geometric and physical criteria. These include reproducing the throat condition $b(r_0) = r_0$, ensuring that the derivative at the throat satisfies $b'(r_0) \leq 1$, and fulfilling both the metric requirement $1 - \frac{b(r)}{r} \geq 0$ ($r > r_0$) and the flare-out condition $\frac{b(r) - rb'(r)}{b^2(r)} > 0$.

A. Case 1:

We begin with the exponential shape function $b(r) = re^{-2(r-r_0)}$. The derivative is found to be $b'(r) = (1 - 2r)\frac{b(r)}{r}$, yielding $\frac{b'(r)}{b(r)} = \frac{1}{r} - 2$. Figure 1 shows that the function and its derivative meet all the geometric criteria required for a physically consistent wormhole and illustrates the embedding surfaces of the wormhole in two and three dimensions, constructed using this shape function. By employing this shape function, one obtains the energy density, radial pressure, and tangential pressure as,

$$\rho = \left[\frac{-2r(3 - 11\varpi_1 + 2\varpi_2) - 12(\varpi_1 + 1)}{(2\varpi_1\varpi_2 + 2\varpi_2 + \varpi_1^2 + 3)(8\pi + 3\ell_1) - 12\ell_1 + 32\pi\varpi_1} \right] \frac{1}{(\xi + 1)r^2 e^{2(r-r_0)}}, \quad (26)$$

$$p_r = \left[\frac{2r(3 - 11\varpi_1 + 2\varpi_2) + 12(\varpi_1 + 1)}{(2\varpi_1\varpi_2 + 2\varpi_2 + \varpi_1^2 + 3)(8\pi + 3\ell_1) - 12\ell_1 + 32\pi\varpi_1} \right] \frac{2\varpi_2 + \gamma}{(\xi + 1)r^2 e^{2(r-r_0)}}, \quad (27)$$

$$p_t = \left[\frac{-2r(3 - 11\varpi_1 + 2\varpi_2) - 12(\varpi_1 + 1)}{(2\varpi_1\varpi_2 + 2\varpi_2 + \varpi_1^2 + 3)(8\pi + 3\ell_1) - 12\ell_1 + 32\pi\varpi_1} \right] \frac{\varpi_2}{(\xi + 1)r^2 e^{2(r-r_0)}}. \quad (28)$$

This work aims to investigate the existence of traversable wormholes that do not require exotic matter within the context of extended gravity theories in the Finsler framework. The present study has examined several scenarios, including one where ϖ_2 is set to -0.465 (Negative, > -1 Quintessence-like in tangential direction), resulting in ϖ_1 taking the value 0.33 (Positive, $\approx 1/3$ Radiation-like in

radial direction). Based on the assumptions stated above and taking $\xi < -1$, the energy density is found to be positive. We now proceed to examine the energy conditions for a wormhole characterized by an exponential shape function as follows,

- NEC:

$$\rho + p_r = \left[\frac{-2r(3 - 11\varpi_1 + 2\varpi_2) - 12(\varpi_1 + 1)}{(2\varpi_1\varpi_2 + 2\varpi_2 + \varpi_1^2 + 3)(8\pi + 3\ell_1) - 12\ell_1 + 32\pi\varpi_1} \right] \frac{1 - (2\varpi_2 + \gamma)}{(\xi + 1)r^2 e^{2(r-r_0)}}, \quad (29)$$

$$\rho + p_t = \left[\frac{-2r(3 - 11\varpi_1 + 2\varpi_2) - 12(\varpi_1 + 1)}{(2\varpi_1\varpi_2 + 2\varpi_2 + \varpi_1^2 + 3)(8\pi + 3\ell_1) - 12\ell_1 + 32\pi\varpi_1} \right] \frac{1 + \varpi_2}{(\xi + 1)r^2 e^{2(r-r_0)}}. \quad (30)$$

$$\begin{cases} \rho + p_r = 1.33\rho \geq 0, \\ \rho + p_t = 0.535\rho \geq 0, \end{cases} \Rightarrow \text{NEC is satisfied}$$

- Weak Energy Condition (WEC):

$$\begin{cases} \rho \geq 0, \\ \rho + p_i \geq 0 \quad \forall i = \{r, t\}. \end{cases} \Rightarrow \text{WEC is satisfied}$$

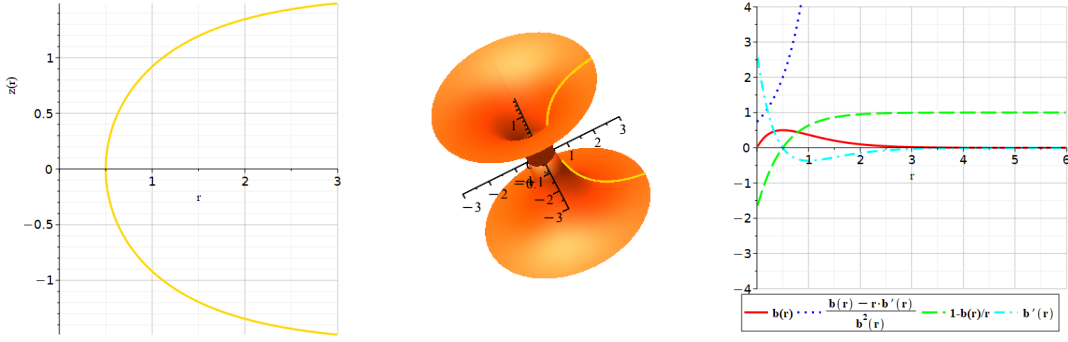


FIG. 1: Embedding surfaces in two and three dimensions constructed from the exponential shape function $b(r) = re^{-2(r-r_0)}$ and its behavior at $r_0 = 0.5$.

- Strong Energy Condition (SEC):

$$\rho + p_r + 2p_t = \left[\frac{-2r(3 - 11\varpi_1 + 2\varpi_2) - 12(\varpi_1 + 1)}{(2\varpi_1\varpi_2 + 2\varpi_2 + \varpi_1^2 + 3)(8\pi + 3\ell_1) - 12\ell_1 + 32\pi\varpi_1} \right] \frac{1 - \gamma}{(\xi + 1)r^2 e^{2(r-r_0)}}, \quad (31)$$

$$\begin{cases} \rho + p_i \geq 0 \quad \forall i = \{r, t\}, \\ \rho + p_r + 2p_t = (1 + 0.08 - 0.68)\rho = 0.4\rho \geq 0. \end{cases} \Rightarrow \text{SEC is satisfied}$$

- Dominant Energy Condition (DEC):

$$\rho - p_r = \left[\frac{-2r(3 - 11\varpi_1 + 2\varpi_2) - 12(\varpi_1 + 1)}{(2\varpi_1\varpi_2 + 2\varpi_2 + \varpi_1^2 + 3)(8\pi + 3\ell_1) - 12\ell_1 + 32\pi\varpi_1} \right] \frac{1 + (2\varpi_2 + \gamma)}{(\xi + 1)r^2 e^{2(r-r_0)}}, \quad (32)$$

$$\rho - p_t = \left[\frac{-2r(3 - 11\varpi_1 + 2\varpi_2) - 12(\varpi_1 + 1)}{(2\varpi_1\varpi_2 + 2\varpi_2 + \varpi_1^2 + 3)(8\pi + 3\ell_1) - 12\ell_1 + 32\pi\varpi_1} \right] \frac{1 - \varpi_2}{(\xi + 1)r^2 e^{2(r-r_0)}}. \quad (33)$$

$$\begin{cases} \rho \geq |p_r| = 0.33\rho, \\ \rho \geq |p_t| = 0.465\rho. \end{cases} \Rightarrow \text{DEC is satisfied}$$

The results obtained in Fig. 2 are significant because they enable a wormhole configuration that does not violate the NEC, indicating that such a structure could be supported by anisotropic, non-exotic matter exhibiting a combination of quintessence-like and radiation-like behavior. This type of fluid could correspond to a generalized anisotropic dark energy model, and due to the NEC being satisfied, exotic matter is not required in this case.

We explored a different range of EoS parameters, $-1 \leq$

$\varpi_2 \leq 0.2$, to identify regions where the NEC is satisfied. The findings, summarized in Table I, indicate that for positive values of ϖ_2 , traversable wormholes satisfying the NEC can exist—unlike in the Riemannian framework [25]. In the Riemannian case, no non-exotic wormhole solutions are found for $\varpi_2 < 0$ down to $\varpi_2 = -0.36$, whereas the Finslerian geometry allows such solutions even in this domain.

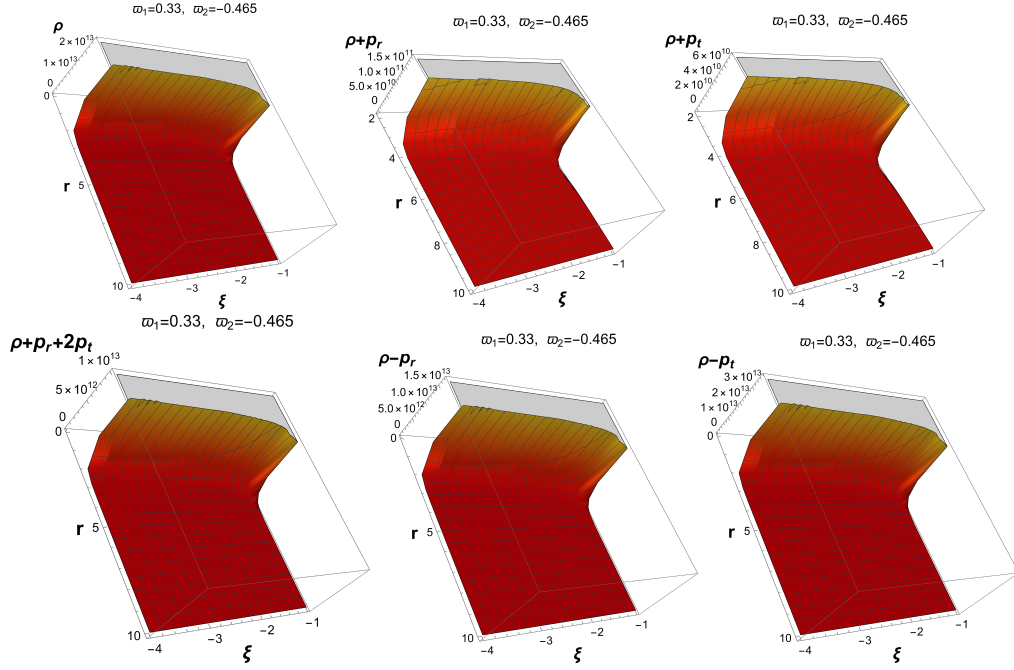


FIG. 2: Satisfaction of all energy conditions (NEC, WEC, SED, DEC) at $r_0 = 0.5$ and $\xi < -1$.

TABLE I: The parameter range of ϖ_2 that ensures the satisfaction of the NEC for the exponential shape function at $r_0 = 0.5$ is identified.

<i>Case 1</i>	ξ	ρ	$\rho + p_r$	$\rho + p_t$	Δp	<i>Case 1</i>	ξ	ρ	$\rho + p_r$	$\rho + p_t$	Δp
$\varpi_2 = 0.195$	$\xi < -1$	+	Positive	Positive	+	$\varpi_2 = 0.175$	$\xi < -1$	+	Positive	Positive	+
$\varpi_2 = 0.155$	$\xi < -1$	+	Positive	Positive	+	$\varpi_2 = 0.12$	$\xi < -1$	+	Positive	Positive	+
$\varpi_2 = 0.105$	$\xi > -1$	+	Positive	Positive	+	$\varpi_2 = 0.10$	$\xi < -1$	+	Positive	Positive	+
$\varpi_2 = -0.13$	$\xi > -1$	+	Positive	Positive	+	$\varpi_2 = -0.15$	$\xi > -1$	+	Positive	Positive	+
$\varpi_2 = -0.165$	$\xi < -1$	+	Positive	Positive	+	$\varpi_2 = -0.17$	$\xi > -1$	+	Positive	Positive	+
$\varpi_2 = -0.18$	$\xi > -1$	+	Positive	Positive	+	$\varpi_2 = -0.2$	$\xi > -1$	+	Positive	Positive	-
$\varpi_2 = -0.215$	$\xi < -1$	+	Positive	Positive	-	$\varpi_2 = -0.22$	$\xi > -1$	+	Positive	Positive	-
$\varpi_2 = -0.24$	$\xi < -1$	+	Positive	Positive	-	$\varpi_2 = -0.25$	$\xi > -1$	+	Positive	Positive	-
$\varpi_2 = -0.255$	$\xi > -1$	+	Positive	Positive	-	$\varpi_2 = -0.26$	$\xi < -1$	+	Positive	Positive	-
$\varpi_2 = -0.265$	$\xi < -1$	+	Positive	Positive	-	$\varpi_2 = -0.28$	$\xi > -1$	+	Positive	Positive	-
$\varpi_2 = -0.295$	$\xi < -1$	+	Positive	Positive	-	$\varpi_2 = -0.305$	$\xi < -1$	+	Positive	Positive	-
$\varpi_2 = -0.315$	$\xi < -1$	+	Positive	Positive	-	$\varpi_2 = -0.335$	$\xi < -1$	+	Positive	Positive	-
$\varpi_2 = -0.34$	$\xi < -1$	+	Positive	Positive	-	$\varpi_2 = -0.355$	$\xi > -1$	+	Positive	Positive	-
$\varpi_2 = -0.365$	$\xi < -1$	+	Positive	Positive	-	$\varpi_2 = -0.37$	$\xi < -1$	+	Positive	Positive	-
$\varpi_2 = -0.38$	$\xi > -1$	+	Positive	Positive	-	$\varpi_2 = -0.39$	$\xi < -1$	+	Positive	Positive	-
$\varpi_2 = -0.43$	$\xi < -1$	+	Positive	Positive	-	$\varpi_2 = -0.435$	$\xi < -1$	+	Positive	Positive	-
$\varpi_2 = -0.44$	$\xi > -1$	+	Positive	Positive	-	$\varpi_2 = -0.445$	$\xi > -1$	+	Positive	Positive	-
$\varpi_2 = -0.45$	$\xi > -1$	+	Positive	Positive	-	$\varpi_2 = -0.455$	$\xi > -1$	+	Positive	Positive	-
$\varpi_2 = -0.465$	$\xi < -1$	+	Positive	Positive	-	$\varpi_2 = -0.58, r > 2.6$	$\xi > -1$	+	Positive	Positive	-
$\varpi_2 = -0.62, r > 2.2$	$\xi > -1$	+	Positive	Positive	-	$\varpi_2 = -0.655, r > 1.9$	$\xi > -1$	+	Positive	Positive	-
$\varpi_2 = -0.685, r > 1.8$	$\xi > -1$	+	Positive	Positive	-	$\varpi_2 = -0.73, r > 1.6$	$\xi < -1$	+	Positive	Positive	-
$\varpi_2 = -0.815, r > 1.4$	$\xi < -1$	+	Positive	Positive	-	$\varpi_2 = -0.825, r > 1.4$	$\xi < -1$	+	Positive	Positive	-
$\varpi_2 = -0.84, r > 1.3$	$\xi > -1$	+	Positive	Positive	-	$\varpi_2 = -0.845, r > 1.3$	$\xi < -1$	+	Positive	Positive	-
$\varpi_2 = -0.855, r > 1.3$	$\xi > -1$	+	Positive	Positive	-	$\varpi_2 = -0.86, r > 1.3$	$\xi > -1$	+	Positive	Positive	-
$\varpi_2 = -0.865, r > 1.3$	$\xi < -1$	+	Positive	Positive	-	$\varpi_2 = -0.87, r > 1.3$	$\xi < -1$	+	Positive	Positive	-
$\varpi_2 = -0.905, r > 1.2$	$\xi > -1$	+	Positive	Positive	-	$\varpi_2 = -0.915, r > 1.2$	$\xi > -1$	+	Positive	Positive	-
$\varpi_2 = -0.925, r > 1.2$	$\xi > -1$	+	Positive	Positive	-	$\varpi_2 = -0.94, r > 1.2$	$\xi < -1$	+	Positive	Positive	-
$\varpi_2 = -0.945, r > 1.2$	$\xi > -1$	+	Positive	Positive	-	$\varpi_2 = -0.965, r > 1.2$	$\xi > -1$	+	Positive	Positive	-
$\varpi_2 = -0.97, r > 1.2$	$\xi < -1$	+	Positive	Positive	-	$\varpi_2 = -0.975, r > 1.2$	$\xi < -1$	+	Positive	Positive	-
$\varpi_2 = -0.985, r > 1.1$	$\xi > -1$	+	Positive	Positive	-	$\varpi_2 = -0.995, r > 1.1$	$\xi > -1$	+	Positive	Positive	-

B. Case 2:

To model the wormhole geometry, we consider a power-law shape function given by $b(r) = \sqrt{r_0 r}$, with its derivative $b'(r) = \frac{\sqrt{r_0}}{2\sqrt{r}}$, leading to $\frac{b'(r)}{b(r)} = \frac{1}{2r}$ [45]. Figure 3

displays the shape function, confirming that it adheres to the required conditions.

Corresponding to this specific shape function, the resulting expressions for energy density, radial pressure, and tangential pressure are found to be,

$$\rho = \frac{-1}{2(\xi + 1)} \left[\frac{27 + 13\varpi_1 + 2\varpi_2}{(2\varpi_1\varpi_2 + 2\varpi_2 + \varpi_1^2 + 3)(8\pi + 3\ell_1) - 12\ell_1 + 32\pi\varpi_1} \right] \sqrt{\frac{r_0}{r^5}}, \quad (34)$$

$$p_r = \frac{2\varpi_2 + \gamma}{2(\xi + 1)} \left[\frac{27 + 13\varpi_1 + 2\varpi_2}{(2\varpi_1\varpi_2 + 2\varpi_2 + \varpi_1^2 + 3)(8\pi + 3\ell_1) - 12\ell_1 + 32\pi\varpi_1} \right] \sqrt{\frac{r_0}{r^5}}, \quad (35)$$

$$p_t = \frac{-\varpi_2}{2(\xi + 1)} \left[\frac{27 + 13\varpi_1 + 2\varpi_2}{(2\varpi_1\varpi_2 + 2\varpi_2 + \varpi_1^2 + 3)(8\pi + 3\ell_1) - 12\ell_1 + 32\pi\varpi_1} \right] \sqrt{\frac{r_0}{r^5}}. \quad (36)$$

In this case, we aim to understand whether traversable wormholes can exist without exotic matter, within the context of extended gravity theories applied in Finsler geometry. One of the studied configurations involves setting $\varpi_2 = -0.465$, which reflects tangential tension similar to that of quintessence, resulting in $\varpi_1 = 0.33$

and indicating mild radial pressure. Under the condition $\xi < -1$, the energy density remains positive. We now investigate the corresponding energy conditions for a wormhole using a power-law shape function similar to case 1.

$$\rho + p_r = \frac{1}{2(\xi + 1)} \left[\frac{(2\varpi_2 + \gamma - 1)(27 + 13\varpi_1 + 2\varpi_2)}{(2\varpi_1\varpi_2 + 2\varpi_2 + \varpi_1^2 + 3)(8\pi + 3\ell_1) - 12\ell_1 + 32\pi\varpi_1} \right] \sqrt{\frac{r_0}{r^5}}, \quad (37)$$

$$\rho + p_t = \frac{1 + \varpi_2}{2(\xi + 1)} \left[\frac{-(27 + 13\varpi_1 + 2\varpi_2)}{(2\varpi_1\varpi_2 + 2\varpi_2 + \varpi_1^2 + 3)(8\pi + 3\ell_1) - 12\ell_1 + 32\pi\varpi_1} \right] \sqrt{\frac{r_0}{r^5}}, \quad (38)$$

$$\rho + p_r + 2p_t = \frac{\gamma - 1}{2(\xi + 1)} \left[\frac{27 + 13\varpi_1 + 2\varpi_2}{(2\varpi_1\varpi_2 + 2\varpi_2 + \varpi_1^2 + 3)(8\pi + 3\ell_1) - 12\ell_1 + 32\pi\varpi_1} \right] \sqrt{\frac{r_0}{r^5}}, \quad (39)$$

$$\rho - p_r = \frac{1}{2(\xi + 1)} \left[\frac{-(2\varpi_2 + \gamma + 1)(27 + 13\varpi_1 + 2\varpi_2)}{(2\varpi_1\varpi_2 + 2\varpi_2 + \varpi_1^2 + 3)(8\pi + 3\ell_1) - 12\ell_1 + 32\pi\varpi_1} \right] \sqrt{\frac{r_0}{r^5}}, \quad (40)$$

$$\rho - p_t = \frac{\varpi_2 - 1}{2(\xi + 1)} \left[\frac{27 + 13\varpi_1 + 2\varpi_2}{(2\varpi_1\varpi_2 + 2\varpi_2 + \varpi_1^2 + 3)(8\pi + 3\ell_1) - 12\ell_1 + 32\pi\varpi_1} \right] \sqrt{\frac{r_0}{r^5}}. \quad (41)$$

Figure 4 illustrates all the energy conditions, indicating that for the selected value of ϖ_2 , the wormhole matter content satisfies the NEC, thus supporting the existence of non-exotic matter wormholes.

We further explored various values of the EoS parameter to identify the specific range for which NEC remains valid. These findings are presented in Table II. In contrast to the Riemannian scenario [25], NEC is satisfied within the range $-0.36 \leq \varpi_2 \leq 0.12$. For $\varpi_2 < -1$, non-exotic matter wormholes are not achievable within this framework of geometry and gravity theory.

C. Anisotropy Factor

Finsler geometry generalizes Riemannian geometry by introducing direction-dependent metrics, leading to more general Einstein-like field equations and effective matter sources. It naturally accommodates anisotropic fluids. Anisotropy exists when $p_r \neq p_t$. $\Delta p = p_t - p_r$, known as the anisotropy factor [46, 47]. The anisotropy in pressure for this wormhole configuration can be written as,

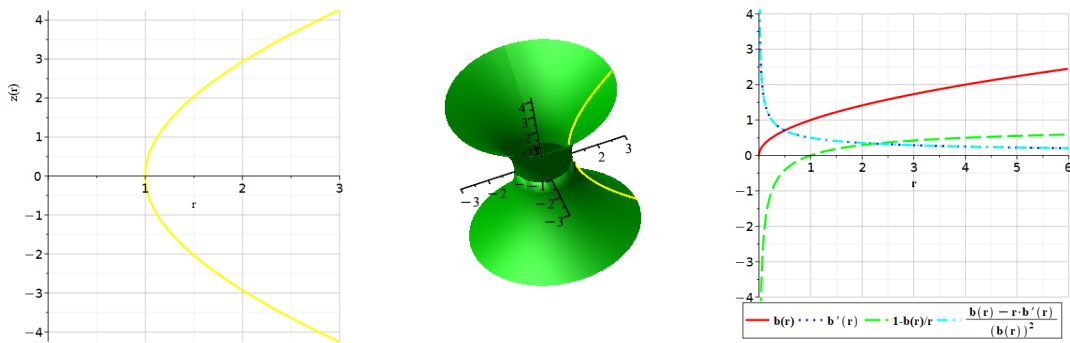


FIG. 3: Embedding surfaces in two and three dimensions constructed from the power-law shape function $b(r) = \sqrt{r_0 r}$ and its behavior at $r_0 = 1$.

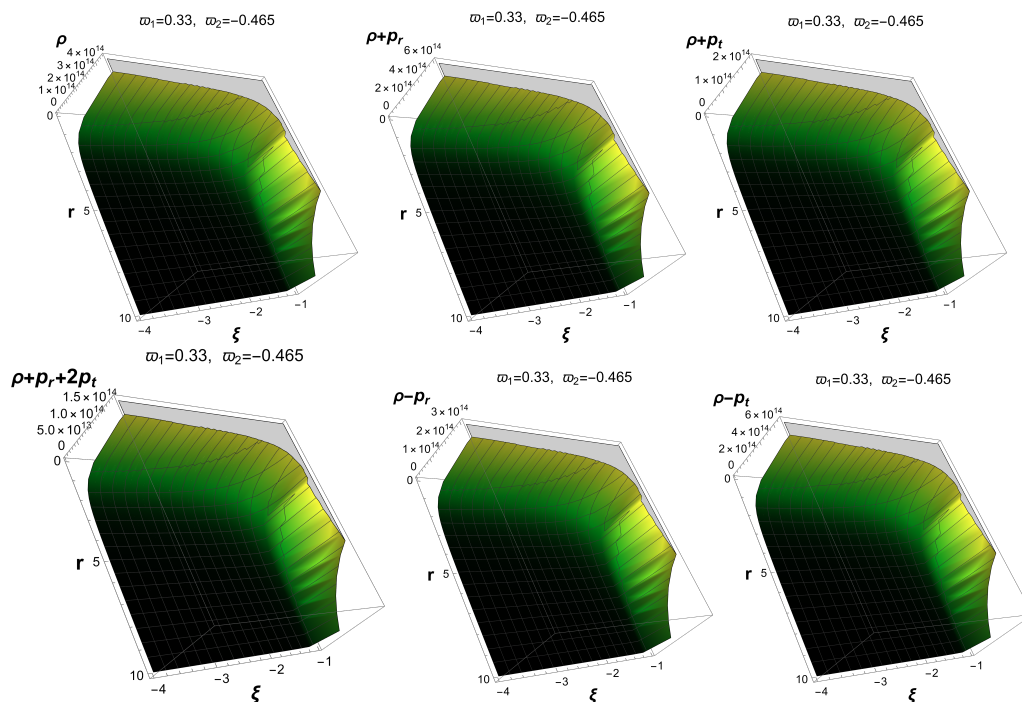


FIG. 4: Satisfaction of all energy conditions (NEC, WEC, SED, DEC) at $r_0 = 1$ and $\xi < -1$.

$$\text{Case 1 : } \Delta p = \left[\frac{-2r(3 - 11\varpi_1 + 2\varpi_2) - 12(\varpi_1 + 1)}{(2\varpi_1\varpi_2 + 2\varpi_2 + \varpi_1^2 + 3)(8\pi + 3\ell_1) - 12\ell_1 + 32\pi\varpi_1} \right] \frac{3\varpi_2 + \gamma}{(\xi + 1)r^2 e^{2(r-r_0)}}, \quad (42)$$

$$\text{Case 2 : } \Delta p = \frac{3\varpi_2 + \gamma}{2(\xi + 1)} \left[\frac{-(27 + 13\varpi_1 + 2\varpi_2)}{(2\varpi_1\varpi_2 + 2\varpi_2 + \varpi_1^2 + 3)(8\pi + 3\ell_1) - 12\ell_1 + 32\pi\varpi_1} \right] \sqrt{\frac{r_0}{r^5}}. \quad (43)$$

From the graphical profile of Δp in Fig. 5, it can be inferred that the wormhole geometry in both cases tends toward an attractive. The tangential pressure is more negative than the radial pressure. This implies that there is stronger tension in the tangential directions, which helps maintain the wormhole throat open. A negative Δp is a

common feature in traversable wormhole solutions — it supports the flaring-out condition configuration.

TABLE II: The parameter range of ϖ_2 that ensures the satisfaction of the NEC for the power-law shape function at $r_0 = 1$ is identified.

<i>Case 2</i>	ξ	ρ	$\rho + p_r$	$\rho + p_t$	Δp	<i>Case 2</i>	ξ	ρ	$\rho + p_r$	$\rho + p_t$	Δp
$\varpi_2 = 0.195$	$\xi < -1$	+	Positive	Positive	+	$\varpi_2 = 0.175$	$\xi < -1$	+	Positive	Positive	+
$\varpi_2 = 0.155$	$\xi < -1$	+	Positive	Positive	+	$\varpi_2 = 0.12$	$\xi < -1$	+	Positive	Positive	+
$\varpi_2 = 0.105$	$\xi > -1$	+	Positive	Positive	+	$\varpi_2 = 0.10$	$\xi < -1$	+	Positive	Positive	+
$\varpi_2 = -0.13$	$\xi > -1$	+	Positive	Positive	+	$\varpi_2 = -0.15$	$\xi > -1$	+	Positive	Positive	+
$\varpi_2 = -0.165$	$\xi < -1$	+	Positive	Positive	+	$\varpi_2 = -0.17$	$\xi > -1$	+	Positive	Positive	+
$\varpi_2 = -0.18$	$\xi > -1$	+	Positive	Positive	+	$\varpi_2 = -0.2$	$\xi > -1$	+	Positive	Positive	-
$\varpi_2 = -0.215$	$\xi < -1$	+	Positive	Positive	-	$\varpi_2 = -0.22$	$\xi > -1$	+	Positive	Positive	-
$\varpi_2 = -0.24$	$\xi < -1$	+	Positive	Positive	-	$\varpi_2 = -0.25$	$\xi > -1$	+	Positive	Positive	-
$\varpi_2 = -0.255$	$\xi > -1$	+	Positive	Positive	-	$\varpi_2 = -0.26$	$\xi < -1$	+	Positive	Positive	-
$\varpi_2 = -0.265$	$\xi < -1$	+	Positive	Positive	-	$\varpi_2 = -0.28$	$\xi > -1$	+	Positive	Positive	-
$\varpi_2 = -0.295$	$\xi < -1$	+	Positive	Positive	-	$\varpi_2 = -0.305$	$\xi < -1$	+	Positive	Positive	-
$\varpi_2 = -0.315$	$\xi < -1$	+	Positive	Positive	-	$\varpi_2 = -0.335$	$\xi < -1$	+	Positive	Positive	-
$\varpi_2 = -0.34$	$\xi < -1$	+	Positive	Positive	-	$\varpi_2 = -0.355$	$\xi > -1$	+	Positive	Positive	-
$\varpi_2 = -0.365$	$\xi < -1$	+	Positive	Positive	-	$\varpi_2 = -0.37$	$\xi < -1$	+	Positive	Positive	-
$\varpi_2 = -0.38$	$\xi > -1$	+	Positive	Positive	-	$\varpi_2 = -0.39$	$\xi < -1$	+	Positive	Positive	-
$\varpi_2 = -0.43$	$\xi < -1$	+	Positive	Positive	-	$\varpi_2 = -0.435$	$\xi < -1$	+	Positive	Positive	-
$\varpi_2 = -0.44$	$\xi > -1$	+	Positive	Positive	-	$\varpi_2 = -0.445$	$\xi > -1$	+	Positive	Positive	-
$\varpi_2 = -0.45$	$\xi > -1$	+	Positive	Positive	-	$\varpi_2 = -0.455$	$\xi > -1$	+	Positive	Positive	-
$\varpi_2 = -0.465$	$\xi < -1$	+	Positive	Positive	-	$\varpi_2 = -0.58$	$\xi < -1$	+	Positive	Positive	-
$\varpi_2 = -0.62$	$\xi < -1$	+	Positive	Positive	-	$\varpi_2 = -0.655$	$\xi < -1$	+	Positive	Positive	-
$\varpi_2 = -0.685$	$\xi < -1$	+	Positive	Positive	-	$\varpi_2 = -0.73$	$\xi > -1$	+	Positive	Positive	-
$\varpi_2 = -0.815$	$\xi > -1$	+	Positive	Positive	-	$\varpi_2 = -0.825$	$\xi > -1$	+	Positive	Positive	-
$\varpi_2 = -0.84$	$\xi < -1$	+	Positive	Positive	-	$\varpi_2 = -0.845$	$\xi > -1$	+	Positive	Positive	-
$\varpi_2 = -0.855$	$\xi < -1$	+	Positive	Positive	-	$\varpi_2 = -0.86$	$\xi < -1$	+	Positive	Positive	-
$\varpi_2 = -0.865$	$\xi > -1$	+	Positive	Positive	-	$\varpi_2 = -0.87$	$\xi > -1$	+	Positive	Positive	-
$\varpi_2 = -0.905$	$\xi < -1$	+	Positive	Positive	-	$\varpi_2 = -0.915$	$\xi < -1$	+	Positive	Positive	-
$\varpi_2 = -0.925$	$\xi < -1$	+	Positive	Positive	-	$\varpi_2 = -0.94$	$\xi > -1$	+	Positive	Positive	-
$\varpi_2 = -0.945$	$\xi < -1$	+	Positive	Positive	-	$\varpi_2 = -0.965$	$\xi < -1$	+	Positive	Positive	-
$\varpi_2 = -0.97$	$\xi > -1$	+	Positive	Positive	-	$\varpi_2 = -0.975$	$\xi > -1$	+	Positive	Positive	-
$\varpi_2 = -0.985$	$\xi < -1$	+	Positive	Positive	-	$\varpi_2 = -0.995$	$\xi < -1$	+	Positive	Positive	-

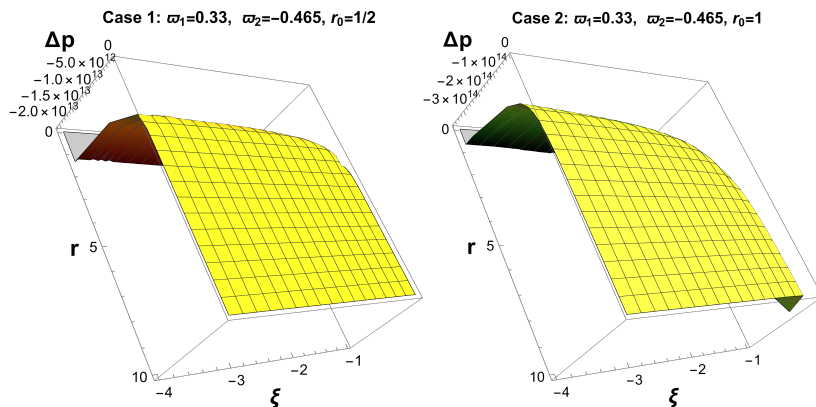


FIG. 5: Depictions of the pressure anisotropy (Δp).

VI. A GEOMETRIC MEASURE OF EXOTICITY IN TRAVERSABLE WORMHOLES

Though quantum effects may allow for NEC violations supporting wormhole throats [48], and such violations are common in GR, alternative gravity theories can permit wormholes sustained entirely by non-exotic matter. This investigation reveals that non-exotic matter wormholes

are attainable for specific intervals of the EoS parameter, highlighting the importance of quantifying the exotic matter contribution. To evaluate the exotic matter contribution, we utilize the following formulation [49, 50]

$$m = 8\pi \oint (p + p_r) dV = 8\pi \int_{r_0}^{\infty} (\rho + p_r) r^2 dr. \quad (44)$$

The radial NEC, $\rho + p_r \geq 0$, is crucial at the wormhole throat $r = r_0$ because the flare-out condition (which ensures a wormhole rather than a black hole or regular geometry) is directly linked to this quantity. A violation of $\rho + p_r \geq 0$ is what typically signals the presence of exotic matter needed to sustain the throat. This integral is valuable to assess whether exotic matter is required near the throat, not just pointwise, but as a net effect, taking the geometry into account. It's crucial for evaluating the physical viability of wormholes in alternative theories of gravity such as Finsler geometry. m can be interpreted as a measure of the effective energy supporting the wormhole, specifically: (1) The active gravitational mass contribution from $\rho + p_r$ over the spatial volume. (2) Sometimes called the "averaged energy condition integral", or a measure of how much non-exoticity (or exoticity) is present.

- If $m < 0$, indicating NEC violation, i.e., exotic matter is required somewhere in the wormhole struc-

ture.

- If $m > 0$, then non-exotic matter is sufficient to support the geometry (at least radially).

A full-range integral $\int_{r_0}^{\infty} (\rho + p_r) dV$ is less informative because (I) it mixes throat behavior with asymptotic regions. (II) Exotic matter, if required, is almost always localized near the throat. (III) Matter becomes normal (or vacuum-like) farther out.

A. Case 1:

While $\rho + p_r > 0$ might hold pointwise in most regions, small NEC-violating zones may still exist near the throat. The volume integral $\int_{r_0}^{r_0+\epsilon} (\rho + p_r) dV$ measures the net effect of such local violations. The result of the integral, when applied to the exponential shape function, is found to be,

$$\begin{aligned}
 m &= 8\pi \int_{r_0}^{r_0+\epsilon} (\rho + p_r) r^2 dr \\
 &= \frac{\left[\epsilon(-6 + 22\varpi_1 - 4\varpi_2) + (-1 + e^{2\epsilon})(15 + \varpi_1 + 2\varpi_2) - 2(-1 + e^{2\epsilon})(-3 + 11\varpi_1 - 2\varpi_2)r_0 \right]}{(\xi + 1)(15 - 12\pi + 8\varpi_1 + 5\varpi_1^2 + 10\varpi_2 + 5\varpi_1\varpi_2)} \\
 &\cdot \left[-e^{-2\epsilon}(1 + \varpi_1) \right], \tag{45}
 \end{aligned}$$

where $\epsilon < 1$. Given a particular choice of the EoS parameter (ϖ_2), the calculation of exotic matter content becomes straightforward. In Fig. 6, we present the exotic mass content for wormholes employing an exponential function, plotted against ϵ . Even though the matter content appears non-exotic locally (due to positive ρ and small p_r), the Finslerian geometric effects (due to $\xi < -1$) near the throat creates a localized region where the volume-integrated radial NEC is violated — effectively behaving like exotic matter is present due to geometry, not due to the EoS. The two-dimensional plots in Fig. 6 are plotted for the specific values mentioned in Table I. The results show that the value of m is positive for values of ϖ_2 that depend on $\xi > -1$. So both local and integrated radial NEC are satisfied. In the vicin-

ity just beyond the throat radius, the wormhole exhibits non-exotic mass content.

B. Case 2:

Integration under the assumption of a power-law shape function leads to [25],

$$\begin{aligned}
 m &= 8\pi \int_{r_0}^{r_0+\epsilon} (\rho + p_r) r^2 dr \\
 &\approx \pi \aleph \sqrt{r_0} \left[8 \left(\frac{\epsilon}{r_0} \right) - 2 \left(\frac{\epsilon}{r_0} \right)^2 + \left(\frac{\epsilon}{r_0} \right)^3 \right], \tag{46}
 \end{aligned}$$

where

$$\aleph = \frac{\sqrt{r_0}}{2(\xi + 1)} \left[\frac{(2\varpi_2 + \gamma - 1)(27 + 13\varpi_1 + 2\varpi_2)}{(2\varpi_1\varpi_2 + 2\varpi_2 + \varpi_1^2 + 3)(8\pi + 3\ell_1) - 12\ell_1 + 32\pi\varpi_1} \right] \tag{47}$$

Figure 7 illustrates the exotic mass content of wormholes

described by a power-law shape function as a function

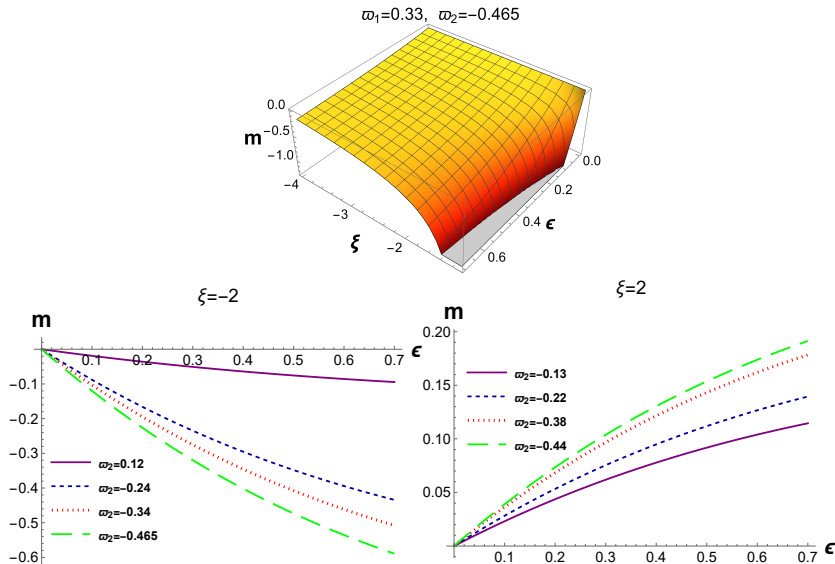


FIG. 6: Exploring exotic matter content corresponding to specific ϖ_2 in the context of an exponential shape function with $r_0 = 1/2$.

of the parameter ϵ . Specific values of ϖ_2 , as listed in Table II—where the NEC holds—have been considered. For each selected ϖ_2 , the exotic mass is predominantly governed by the linear term, displaying an almost linear increase with rising ϵ . Moreover, in regions slightly offset from the wormhole throat, the exotic mass content approaches zero. In this case, unlike case 1, where only the value of m for ϖ_2 is positive depending on $\xi > -1$, it is positive for all the cases mentioned in Table II.

VII. CONCLUSIONS

This study presents a rigorous investigation into traversable wormholes that can be sustained without exotic matter within squared-trace extended gravity $f(\mathbb{R}, \mathbb{T})$, embedded in Finsler-Randers geometry with the Barthel connection. By exploiting the inherent anisotropy of Finsler space-times, where the metric decomposes into a Riemannian component $\alpha(x, y)$ and a 1-form $\beta(x, y)$, we demonstrated that direction-dependent pressures can naturally emerge in the gravitational sector.

A novel insight is that Finslerian anisotropy generates effective stresses, which are crucial for satisfying the flaring-out condition at the wormhole throat without invoking exotic matter. We showed that barotropic equations of state $p_r = \varpi_1 \rho$ and $p_t = \varpi_2 \rho$ yield explicit parametric regimes—such as $\varpi_1 \approx 1/3$ and $\varpi_2 \in (-1, -1/3)$ —where all classical energy conditions (NEC, WEC, SEC, DEC) are simultaneously fulfilled. We found that radiation-like behavior in the radial direction ensures positive radial pressure, while quintessence-like behavior in the tangential direction provides negative pres-

sure that stabilizes the throat.

We demonstrated that both exponential and power-law shape functions produce geometrically regular wormholes, free of horizons and characterized by positive energy densities. Our analysis further showed that the exoticity integral $\oint (\rho + p_r) dV$ remains positive over a wide range of parameters, confirming the physical viability of these solutions. Compared to earlier Riemannian $f(\mathbb{R}, \mathbb{T})$ wormhole studies [25], the present Finslerian construction admits NEC-satisfying solutions for significantly wider ranges of the tangential equation-of-state parameter ϖ_2 , including domains that are inaccessible in the Riemannian limit.

Overall, we established that the synergy between squared-trace gravity and Finsler-Randers geometry provides a robust theoretical framework for constructing traversable wormholes supported by realistic matter. This work opens new pathways for anisotropic gravitational modeling and advances the prospect of wormholes as viable astrophysical and cosmological constructs.

In future research, generalizing the framework to include other alternative theories of gravity, such as $f(\mathbb{Q}, \mathbb{T})$ or teleparallel equivalents, could broaden the parameter space for physically realistic wormhole models. Finally, exploring the interplay between Finslerian anisotropies and dark energy components may offer new perspectives on unifying wormhole physics with large-scale cosmic acceleration.

ACKNOWLEDGEMENTS

The work of KB was supported in part by the JSPS KAKENHI Grant Numbers 24KF0100, 25KF0176 and

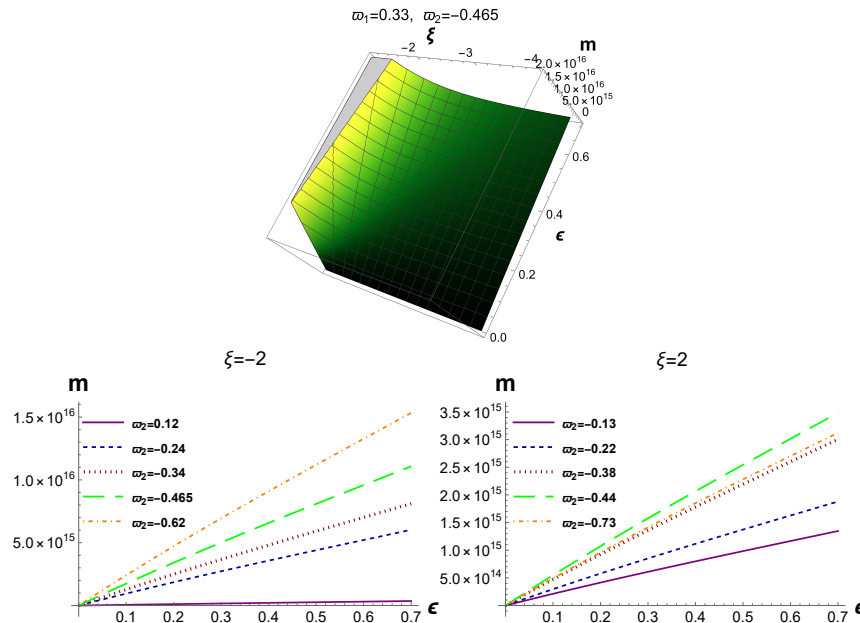


FIG. 7: Exploring exotic matter content corresponding to specific ϖ_2 in the context of a power-law shape function with $r_0 = 1$.

Competitive Research Funds for Fukushima University Faculty (25RK011).

-
- [1] M.S. Morris, K.S. Thorne, Wormholes in spacetime and their use for interstellar travel: A tool for teaching general relativity, *Am. J. Phys.* **56**, 395–412 (1988). <https://doi.org/10.1119/1.15620>.
- [2] M. Visser, *Lorentzian Wormholes: From Einstein to Hawking*, AIP Press, New York, 1995.
- [3] D. Hochberg, M. Visser, Geometric structure of the generic static traversable wormhole throat, *Phys. Rev. D* **56**, 4745 (1997). <https://doi.org/10.1103/PhysRevD.56.4745>.
- [4] M. Visser, Traversable wormholes from surgically modified Schwarzschild spacetimes, *Nucl. Phys. B* **328**, 203–212 (1989). [https://doi.org/10.1016/0550-3213\(89\)90100-4](https://doi.org/10.1016/0550-3213(89)90100-4).
- [5] F.S.N. Lobo (Ed.), *Wormholes, Warp Drives and Energy Conditions*, (Fundamental Theories of Physics, 189), Springer, 2017. <https://doi.org/10.1007/978-3-319-55182-1>.
- [6] T. Padmanabhan, Dark energy and gravity, *Gen. Rel. Grav.* **40**, 529–564 (2008). <https://doi.org/10.1007/s10714-007-0555-7>.
- [7] R. Durrer, R. Maartens, Dark Energy and Dark Gravity: theory overview, *Gen. Rel. Grav.* **40**, 301–328 (2008). <https://doi.org/10.1007/s10714-007-0549-5>.
- [8] T.P. Sotiriou, V. Faraoni, $f(R)$ theories of gravity, *Rev. Mod. Phys.* **82**, 451–497 (2010). <https://doi.org/10.1103/RevModPhys.82.451>.
- [9] A. De Felice, S. Tsujikawa, $f(R)$ Theories, *Living Rev. Rel.* **13**, 3 (2010). <https://doi.org/10.12942/lrr-2010-3>.
- [10] S. Nojiri and S.D. Odintsov, Unified cosmic history in modified gravity: from $F(R)$ theory to Lorentz non-invariant models, *Phys. Rept.* **505**, 59–144 (2011). <https://doi.org/10.1016/j.physrep.2011.04.001>.
- [11] S. Capozziello, M. De Laurentis, Extended Theories of Gravity, *Phys. Rept.* **509**, 167–321 (2011). <https://doi.org/10.1016/j.physrep.2011.09.003>.
- [12] T. Clifton, P.G. Ferreira, A. Padilla, C. Skordis, Modified Gravity and Cosmology, *Phys. Rept.* **513**, 1–189 (2012). <https://doi.org/10.1016/j.physrep.2012.01.001>.
- [13] S. Nojiri, S.D. Odintsov, V.K. Oikonomou, Modified Gravity Theories on a Nutshell: Inflation, Bounce and Late-time Evolution, *Phys. Rept.* **692**, 1–104 (2017). <https://doi.org/10.1016/j.physrep.2017.06.001>.
- [14] V. De Falco, E. Battista, S. Capozziello et al. Reconstructing wormhole solutions in curvature based Extended Theories of Gravity, *Eur. Phys. J. C* **81**, 157 (2021). <https://doi.org/10.1140/epjc/s10052-021-08958-4>.
- [15] T. Harko, F.S.N. Lobo, S. Nojiri, S.D. Odintsov, $f(R, T)$ gravity, *Phys. Rev. D* **84**, 024020 (2011). <https://doi.org/10.1103/PhysRevD.84.024020>.
- [16] P.H.R.S. Moraes, P.K. Sahoo, Nonexotic matter wormholes in a trace of the energy-momentum tensor squared gravity, *Phys. Rev. D* **97**, 024007 (2018). <https://doi.org/10.1103/PhysRevD.97.024007>.
- [17] M. Zubair, S. Waheed, Y. Ahmad, Static spherically symmetric wormholes in $f(R, T)$ gravity, *Eur. Phys. J. C* **76**, 444 (2016). <https://doi.org/10.1140/epjc/s10052-016-4288-1>.
- [18] J. Luís Rosa, P.M. Kull, Non-exotic traversable wormhole solutions in linear $f(R, T)$ gravity, *Eur. Phys. J. C* **82**, 1154 (2022). <https://doi.org/10.1140/epjc/s10052-022-11135-w>.
- [19] R.A.C. Cipriano, N. Ganiyeva, T. Harko, F.S.N. Lobo, M.A.S. Pinto, J. Luís Rosa, Energy-Momentum Squared Gravity: A Brief Overview, *Universe* **10**(9), 339 (2024). <https://doi.org/10.3390/universe10090339>.

- [20] C.V.R. Board, J.D. Barrow, Cosmological Models in Energy-Momentum-Squared Gravity, *Phys. Rev. D* **96**, 123517 (2017). <https://doi.org/10.1103/PhysRevD.96.123517>.
- [21] N. Nari, M. Roshan, Compact stars in Energy-Momentum Squared Gravity, *Phys. Rev. D* **98**, 024031 (2018). <https://doi.org/10.1103/PhysRevD.98.024031>.
- [22] Ö. Akarsu, J.D. Barrow, S.Çikintoğlu, K.Y. Ekşi, N. Katirci, Constraint on energy-momentum squared gravity from neutron stars and its cosmological implications, *Phys. Rev. D* **97**, 124017 (2018). <https://doi.org/10.1103/PhysRevD.97.124017>.
- [23] F. Parsaei, S. Rastgoo, Wormholes in $f(R, T) = R + \lambda T + \lambda_1 T^2$ gravity, *Commun. Theor. Phys.* **78**, 025403 (2026). <https://doi.org/10.1088/1572-9494/ae0159>.
- [24] M. Sharif, M. Zeeshan Gul, Viable wormhole solutions in energy-momentum squared gravity, *Eur. Phys. J. Plus* **136**, 503 (2021). <https://doi.org/10.1140/epjp/s13360-021-01512-x>.
- [25] S.K. Tripathy, D. Nayak, B. Mishra, D. Behera, S.K. Sahu, Existence of non-exotic traversable wormholes in squared trace extended gravity theory, *Nucl. Phys. B* **1001**, 116513 (2024). <https://doi.org/10.1016/j.nuclphysb.2024.116513>.
- [26] M. Roshan, F. Shojai, Energy-momentum squared gravity, *Phys. Rev. D* **94**, 044002 (2016). <https://doi.org/10.1103/PhysRevD.94.044002>.
- [27] P.H.R.S. Moraes, José D.V. Arbañil, M. Malheiro, Stellar equilibrium configurations of compact stars in $f(R, T)$ theory of gravity, *J. Cosmol. Astropart. Phys.* **2016**(06), 005 (2016). <https://doi.org/10.1088/1475-7516/2016/06/005>.
- [28] M. Zubair, Q. Muneer, S. Waheed, Traversable Wormholes Existence in $f(R, T)$ Gravity Involving Trace-Squared Term with Nonexotic Matter, *Adv. Astron.* **2021**, 680069 (2021). <https://doi.org/10.1155/2021/6680069>.
- [29] A. Bouali, H. Chaudhary, L. Csillag, R. Hama, T. Harko, Sorin V. Sabau, S. Shahidi, From Barthel–Randers–Kropina Geometries to the Accelerating Universe: A Brief Review of Recent Advances in Finslerian Cosmology, *Universe* **11**, 198 (2025). <https://doi.org/10.3390/universe11070198>.
- [30] Z. Nekouee, S.K. Narasimhamurthy, T. Sanjay, B.R. Yashwanth, M. Malligawad, Geometry-driven wormholes in Barthel-Randers space-time under generalized Rastall framework, *Nucl. Phys. B* **1018**, 117066 (2025). <https://doi.org/10.1016/j.nuclphysb.2025.117066>.
- [31] R. Hama, T. Harko, S.V. Sabau, Dark energy and accelerating cosmological evolution from osculating Barthel–Kropina geometry, *Eur. Phys. J. C* **82**, 385 (2022). <https://doi.org/10.1140/epjc/s10052-022-10318-9>.
- [32] M. Matsumoto, Theory of Finsler spaces with (α, β) -metric, *Rep. Math. Phys.* **31**, 43–83 (1992). [https://doi.org/10.1016/0034-4877\(92\)90005-L](https://doi.org/10.1016/0034-4877(92)90005-L).
- [33] V.S. Sabau, H. Shimada, Classes of Finsler spaces with (α, β) -metrics, *Rep. Math. Phys.* **47**, 31–48 (2001). [https://doi.org/10.1016/S0034-4877\(01\)90004-7](https://doi.org/10.1016/S0034-4877(01)90004-7).
- [34] P.C. Stavrinou, A.P. Kouretsis, FRW-metric and Friedmann equations in a generalized cosmological model, *J. Phys.: Conf. Ser.* **68**, 012023 (2007). <https://doi.org/10.1088/1742-6596/68/1/012023>.
- [35] R.S. Ingarden, M. Matsumoto, On the 1953 Barthel connection of a Finsler space and its mathematical and physical interpretation, *Rep. Math. Phys.* **32**, 35–48 (1993). [https://doi.org/10.1016/0034-4877\(93\)90070-U](https://doi.org/10.1016/0034-4877(93)90070-U).
- [36] R.S. Ingarden, Vector field relative Finsler space in two physical examples, *Nonlinear World* **04**, 85–100 (1997).
- [37] R.S. Ingarden, L. Tamassy, The point Finsler spaces and their physical applications in electron optics and thermodynamics, *Math. Comput. Model.* **20**, 93–107 (1994). [https://doi.org/10.1016/0895-7177\(94\)90159-7](https://doi.org/10.1016/0895-7177(94)90159-7).
- [38] R. Hama, T. Harko, S.V. Sabau, S. Shahidi, Cosmological evolution and dark energy in osculating Barthel–Randers geometry, *Eur. Phys. J. C* **81**, 742 (2021). <https://doi.org/10.1140/epjc/s10052-021-09517-7>.
- [39] B.R. Yashwanth, S.K. Narasimhamurthy, J. Praveen, M. Malligawad, The influence of density models on wormhole formation in Finsler–Barthel–Randers geometry, *Eur. Phys. J. C* **84**, 1272 (2024). <https://doi.org/10.1140/epjc/s10052-024-13541-8>.
- [40] J. Praveen, S.K. Narasimhamurthy, Developing novel wormhole metrics in Finsler-Randers geometry using the Barthel connection and Osculating-Riemannian method, *Phys. Scr.* **99**, 105251 (2024). <https://doi.org/10.1088/1402-4896/ad7709>.
- [41] R.A. Konoplya, How to tell the shape of a wormhole by its quasinormal modes, *Phys. Lett. B* **784**, 43–49 (2018). <https://doi.org/10.1016/j.physletb.2018.07.025>.
- [42] M. Hohmann, Traversable wormholes without exotic matter in multimetric repulsive gravity, *Phys. Rev. D* **89**, 087503 (2014). <https://doi.org/10.1103/PhysRevD.89.087503>.
- [43] P.D. Krishna, D. Ujjal, Possible existence of traversable wormhole in Finsler-Randers geometry, *Eur. Phys. J. C* **83**, 821 (2023). <https://doi.org/10.1140/epjc/s10052-023-11910-3>.
- [44] T. Sanjay, S.K. Narasimhamurthy, Z. Nekouee, H.M. Manjunatha, Traversable wormhole models in Finslerian geometry, *Pramana- J. Phys.* **98**, 16 (2024). <https://doi.org/10.1007/s12043-023-02718-7>.
- [45] E. Elizalde, M. Khurshudyan, Wormholes with $\rho(R, R')$ matter in $f(R, T)$ gravity, *Phys. Rev. D* **99**, 024051 (2019). <https://doi.org/10.1103/PhysRevD.99.024051>.
- [46] F. Rahaman, M. Kalam, K.A. Rahman, Wormhole Geometry from Real Feasible Matter Sources, *Int. J. Theor. Phys.* **48**, 471–475 (2009). <https://doi.org/10.1007/s10773-008-9822-y>.
- [47] M. Sharif, S. Saba, Gravitational Decoupled Anisotropic Solutions in $f(G)$ Gravity, *Eur. Phys. J. C* **78**, 921 (2018). <https://doi.org/10.1140/epjc/s10052-018-6406-8>.
- [48] D. Hochberg, M. Visser, Null Energy Condition in Dynamic Wormholes, *Phys. Rev. Lett.* **81**, 746 (1998). <https://doi.org/10.1103/PhysRevLett.81.746>.
- [49] S.K. Tripathy, Modelling Casimir wormholes in extended gravity, *Phys. Dark Universe* **31**, 100757 (2021). <https://doi.org/10.1016/j.dark.2020.100757>.
- [50] M. Visser, S. Kar, N. Dadhich, Traversable Wormholes with Arbitrarily Small Energy Condition Violations, *Phys. Rev. Lett.* **90**, 201102 (2003). <https://doi.org/10.1103/PhysRevLett.90.201102>.